SynBio

MDPI

Article

Chemo-Enzymatic Synthesis of Bioactive Carbazole Derivatives

Saad Alrashdi [1,2,†], Federica Casolari [1,†], Kwaku Kyeremeh [3] and Hai Deng [1,*]

[1] Department of Chemistry, University of Aberdeen, Aberdeen AB24 3UE, UK; s.alrashdi.18@abdn.ac.uk (S.A.); federica.casolari@abdn.ac.uk (F.C.)
[2] College of Science and Arts in Gurayat, Jouf University, King Khaled Road, Sakakah, Saudi Arabia
[3] Marine and Plant Research Laboratory of Ghana, Department of Chemistry, University of Ghana, Legon-Accra P.O. Box LG56, Ghana; kkyeremeh@ug.edu.gh
* Correspondence: h.deng@abdn.ac.uk
† These authors contributed equally to this work.

Abstract: Carbazoles are key scaffolds of either antimicrobial/antiviral alkaloid natural products or therapeutics. As such, access to structurally diverse indole-containing carbazoles has attracted considerable attention. In this report, a pilot study is described using biotransformation to provide carbazoles that contain various acyl substituents. The biotransformation system contains the thiamine-diphosphate (ThDP)-dependent enzyme NzsH, the FabH-like 3-ketoacyl-ACP synthase NzsJ, and the aromatase/cyclase NzsI, encoded in the biosynthetic gene cluster (*nzs*) of the bacterial carbazole alkaloid natural product named neocarazostatin A. The utilization of a range of acyl-SNACs (synthetic acyl-thioester analogues of the native substrate) together with indole-3-pyruvate and pyruvate in the designed biotransformation system allows production of carbazole derivatives. Our results demonstrate that this three-enzyme system displays a considerable substrate profile toward acyl donors for production of carbazoles with different acyl substituents. Finally, two more enzymes were included in the biotransformation system: the tryptophan synthase stand-alone β-subunit variant, *Pf*TrpB, generated from directed evolution in the literature, and a commercially available L-amino acid oxidase (LAAO). The addition of these two enzymes allows the transformation to start with indole building blocks to provide carbazoles with modifications in the indole ring system.

Keywords: alkaloid natural products; chemo-enzymatic reaction; one-pot biotransformation; biosynthesis

Citation: Alrashdi, S.; Casolari, F.; Kyeremeh, K.; Deng, H. Chemo-Enzymatic Synthesis of Bioactive Carbazole Derivatives. *SynBio* **2024**, *2*, 21–30. https://doi.org/10.3390/synbio2010002

Academic Editor: Masahito Yamagata

Received: 18 October 2023
Revised: 14 November 2023
Accepted: 27 December 2023
Published: 4 January 2024

1. Introduction

Carbazoles consist of a tricyclic backbone with two benzene rings fused through the formation of a pyrrole ring (Figure 1). Carbazole-containing molecules have applications in chemical industries (e.g., the dye material pigment violet 23) **1** or are currently used as therapeutics (e.g., the anti-inflammatory drug carprofen) **2**, as shown in Figure 1A. Furthermore, these heterocycles also serve as key building blocks for the design of organic light-emitting diode (OLED) materials and photoconductors due to their wide band gap and promising optoelectronic properties [1–5].

Therefore, there has been a considerable amount of research into the development of facile but efficient methods to access these privileged heterocyclic scaffolds. Although there exists a plethora of synthetic approaches to producing carbazoles, these protocols often entail the use of multiple steps, require harsh reaction conditions, are restricted to specific starting materials, use precious metal catalysts, and require either stoichiometric amounts of expensive oxidants or dehydrogenating agents.

Naturally occurring carbazole alkaloids (CAs) are mainly produced by higher plants and fungi [6]. However, the bio-origin of these natural products remains elusive. In contrast to CAs from higher plants and fungi, bacterial CAs are much less common, which include bis-indole CAs, such as staurosporine and rebeccamycin, and indolosesquiterpenes [7–10]. Apart from these structurally complex CAs, some bacteria also produce a

rather simple tricyclic ring system with aliphatic side chains, including carquinostatins, carazostatin, carbazoquinocins, carbazomycin, (*S*)-streptoverticillin, and neocarazostatins (Figure 1) [11–16]. Generally, this group of bacterial carbazoles act as antibacterial agents and free radical scavengers with potent neuronal cell-protecting activity.

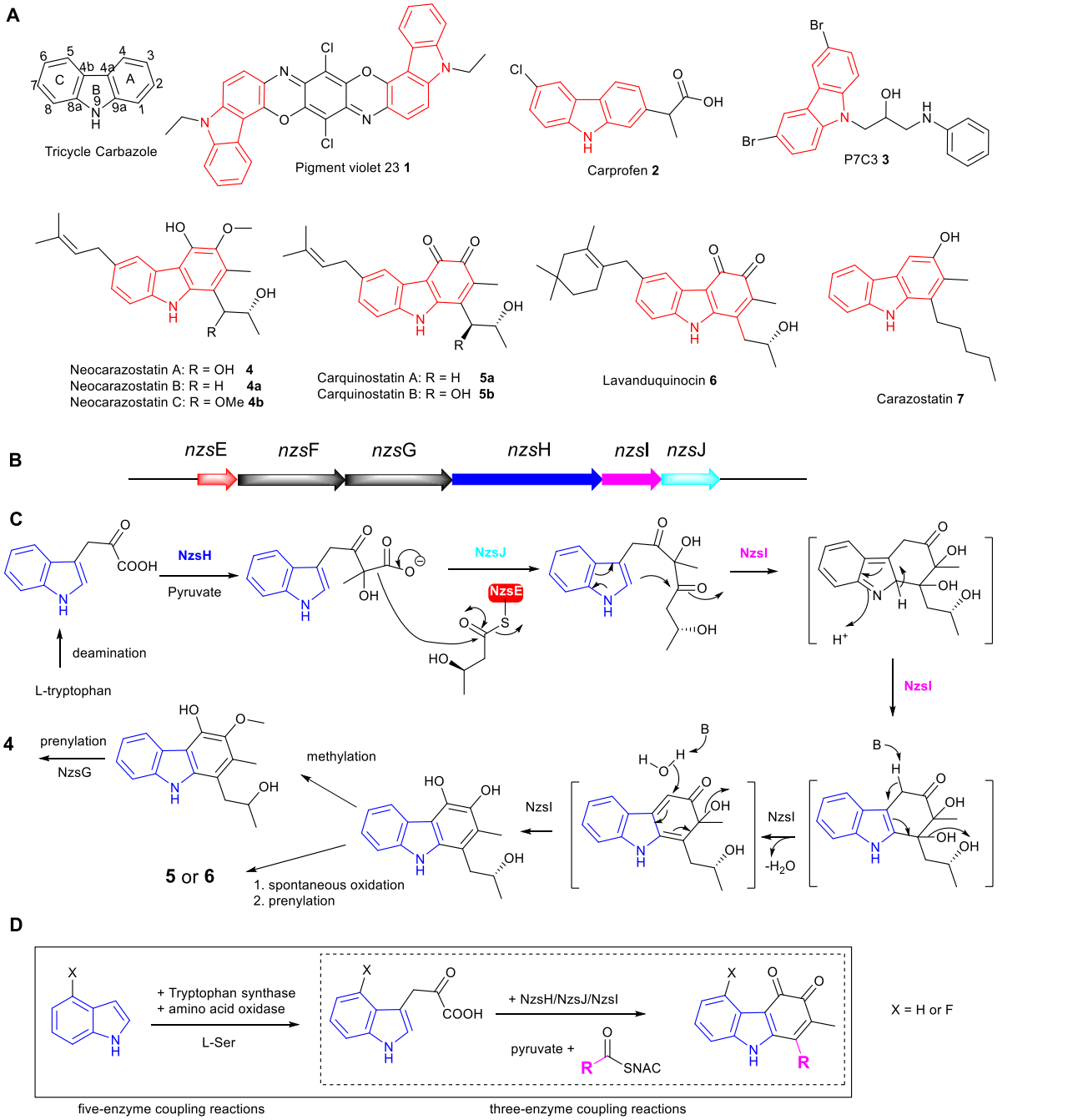

Figure 1. (**A**) Representative structures of tricyclic carbazole, utility molecules containing carbazole motifs, and one group of bacterial metabolites containing simple carbazole scaffolds. (**B**) The conserved essential genes responsible for the production of this group of bacterial carbazoles. The conserved genes are color-coded. *nzs*E: red, *nzs*H: blue, *nzs*I: pink, and *nzs*J: light blue. (**C**) The proposed pathways of bacterial carbazoles starting from indole-3-pyruvate catalyzed by three enzyme homologues (NzsH, NzsJ and NzsI in the case of 4). The corresponding conserved enzymes are color-coded. NzsE: red, NzsH: blue, NzsI: pink, and NzsJ: light blue. (**D**) Chemo-enzymatic synthesis of structurally diverse carbazole molecules in this study.

Recently, our research group has been actively involved in the characterization of the biosynthetic pathways of two bacterial carabazoles: neocarazostatin A **3** and carquinostatin **4** (Figure 1B) [17–19]. The biosynthetic gene clusters of CAs encode highly conserved enzymes: a standalone acyl carrier protein (NzsE in case of **3**), a thiamine diphosphate-dependent enzyme (NzsH), a FabH-like 3-ketoacyl-ACP synthase (KAS) III (NzsJ), and the aromatase/cyclase (NzsI). Pathway reconstitution of these CAs demonstrated that NzsH and its homologues catalyze the first carboligation between indole-3-pyruvate and pyruvate to generate the indole-containing acyloin intermediate. Subsequently, NzsJ and its homologues mediate a decarboxylation-driven condensation with a protein-tethered fatty acid moiety, followed by cyclization and water-based nucleophilic aromatization by the aromatase/cyclase NzsI to yield the key catechol-type intermediate, which would undergo spontaneous oxidation to provide *ortho*-quinone types of CAs (Figure 1C) [20–23]. It was demonstrated that NzsH displays considerable substrate promiscuity towards different indole moieties to generate acyloin derivatives with structural diversity. This was achieved through a one-pot biotransformation system containing an engineered tryptophane synthase β-subunit, a commercially available L-amino acid oxidase, and NzsH [24].

Herein, a pilot study of new coupled biotransformation protocols to access CA derivatives is reported using three-enzyme or five-enzyme systems. In the three-enzyme system, the reaction is initiated with indole-pyruvate and pyruvate catalyzed by NzsH to generate the transient acyloin intermediate, which will subsequently be converted into CA derivatives in the presence of NzsJ and NzsI, together with acyl-SNACs, synthetic acyl thioester donors of the natural substrate (Figure 1D). Among the acyl-SNACs, the best substrate for the coupled system of NzsJ and NzsI is isovaleryl-SNAC based on the interpretation of ion absorptions of the corresponding CAs under the same enzymatic conditions. Further substrate tolerance of indole derivatives is explored in the five-enzyme system, including NzsJ and NzsI together with NzsH, the engineered tryptophan synthase *Pf*TrpB, and the amino acid oxidase, as previously reported (Figure 1D). Among the indole derivatives examined, only 4-fluoro-indole can pass the five-enzyme system to finally generate a 4-fluoro-CA derivative when *iso*-valeryl-SNAC is used, suggesting that NzsJ and NzsI display a certain degree of substrate specificity on the indole moieties. Further enzyme engineering is needed to expand the substrate plasticity of NzsJ and NzsI to fully appreciate their catalytic capacity.

2. Result and Discussion

To generate structurally diverse CA derivatives, acyl and indole derivatives with structural diversity are key to evaluating the substrate plasticity of NzsJ and NzsI. The previous studies indicated that the NzsJ and NzsI homologues in the biosynthesis of carquinostatins **5** were able to integrate acyl-CoAs into the CA frameworks. N-Acetylcysteamine (SNAC) is commonly used as a simplified synthetic mimic of reactive biosynthetic intermediates such as acyl-ACP in biosynthetic studies. This is particularly useful when the availability of acyl-CoAs with structural diversity is limited. Our previously conducted study demonstrated that the acyl-ACP derivative 3-hydroxybutyryl-SNAC can be incorporated into neocarazostatin A in our pathway reconstitution studies, indicating that NzsJ and NzsI can accept synthetic SNAC surrogates [21]. To this end, ten synthetic acyl-SNACs were acquired from our previous studies [25,26] (Figure S1) to examine whether these compounds can enter the CA scaffold. The synthetic constructs were overexpressed, containing the genes *nzs*J and *nzs*I, in *E. coli* BL21 (DE3). Both recombinant NzsJ and NzsI were expressed with N-terminal pHis6 tags and were purified to near homogenesis by Ni-NTA chromatography, yielding estimated molecular weights of 35.0 and 28.0 Da, respectively, as previously reported (Figure S2) [21]. Inclusion of NzsJ (40 μM) and NzsI (40 μM) into the reaction of NzsH (20 μM), together with TPP and Mg^{2+} and isovaleryl-SNACs (1 mM), resulted in the formation of an isovaleryl-containing CA derivative with a m/z value of 268.1330 (mass error: 0.7 ppm, calculated m/z = 268.1332), as evidenced in HPLC analysis (Figure 2B) and LC high-resolution MS (LC-HRMS) (Figure S3), respectively.

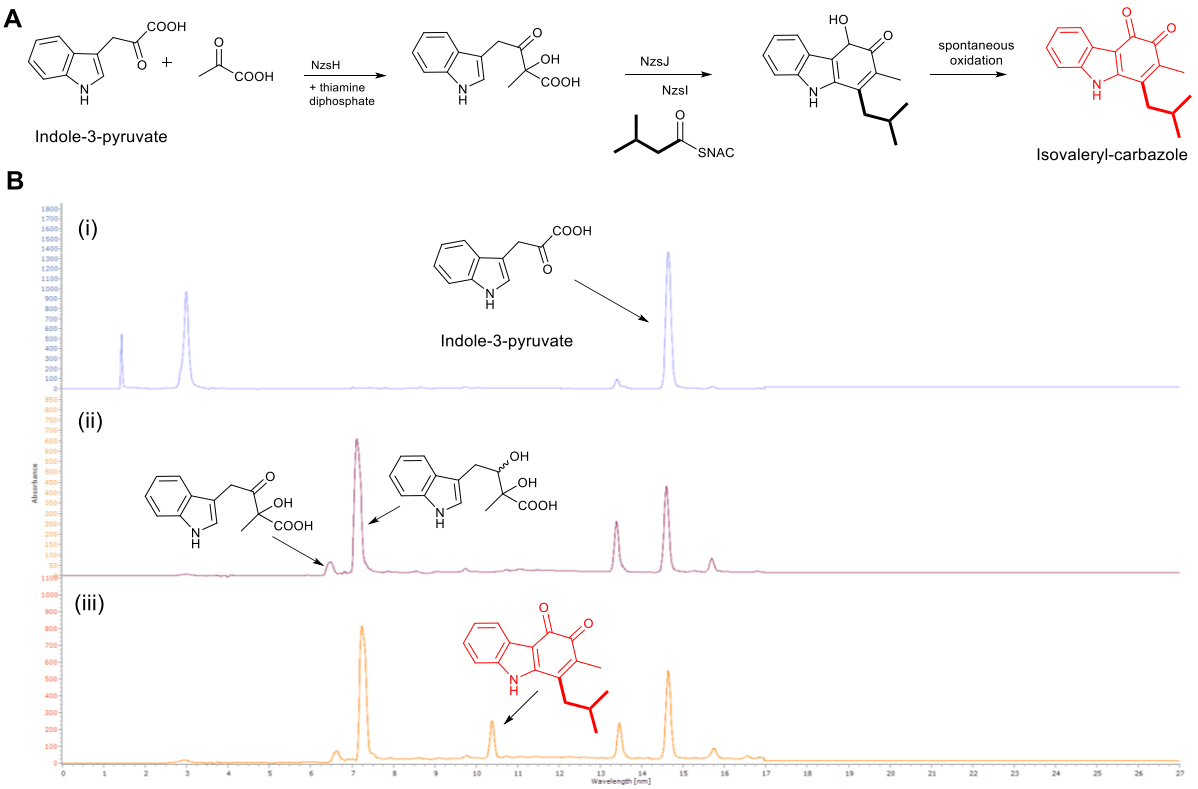

Figure 2. HPLC analysis confirming production of iso-valeryl carbazole (CA) derivative. (**A**) A biotransformation scheme starting from indole-3-pyruvate and pyruvate together with isovaleryl-SNAC to generate isovaleryl-CAs. (**B**) HPLC traces of the biotransformation from indole-3-pyruvate and pyruvate together with isovaleryl-SNACs to isovaleryl-CA. (i). indole-3-pyruvate as a control. (ii). The production of acyloins generated by NzsH-catalyzed system. (iii). The production of isovaleryl-CA generated by the three-enzyme biotransformation system, including NzsH, J, and I.

Encouraged by the results of this three-enzyme coupling system, the remaining nine acyl-SNAC derivatives were further investigated (Table 1). Our LC-MS and tandem MS analyses demonstrated that all of these acyl-SNACs can be transformed into the corresponding CA derivatives (Table 1 and Figures S4–S12) in the corresponding coupled chemo-enzymatic systems.

Table 1. Acyl-carbazole derivatives generated in this study from structurally diverse substrates, acyl-SNACs. Results are shown as exact mass of protonated ion $[M+H]^+$ (mass error in ppm).

Acyl-SNAC	⟹	**Acyl-Carbazoles**
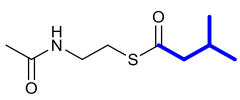 Exact mass = 204.1053 m/z (0.1 ppm)	⟹	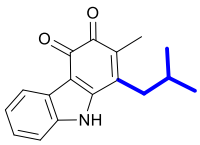 Exact mass = 268.1332 m/z (0.7 ppm)
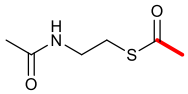 Exact mass = 162.0583 m/z (0.7 ppm)	⟹	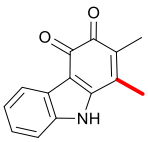 Exact mass = 226.0863 m/z (3.8 ppm)

Table 1. *Cont.*

Acyl-SNAC		Acyl-Carbazoles
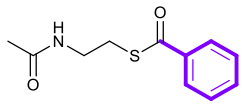 Exact mass = 224.0740 m/z (0.1 ppm)	⟹	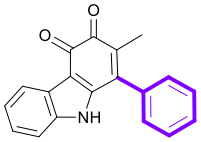 Exact mass = 288.1019 m/z (0.1 ppm)
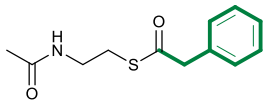 Exact mass = 238.0897 m/z (0.2 ppm)	⟹	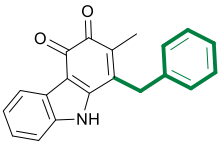 Exact mass = 302.1176 m/z (0.0 ppm)
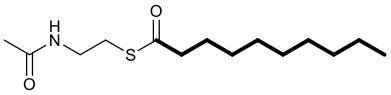 Exact mass = 274.1835 m/z (0.2 ppm)	⟹	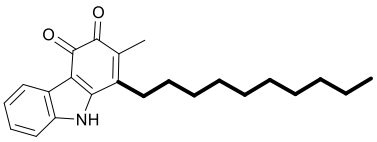 Exact mass = 338.2115 m/z (0.3 ppm)
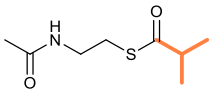 Exact mass = 188.0745 m/z (0.7 ppm)	⟹	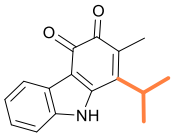 Exact mass = 254.1176 m/z (1.0 ppm)
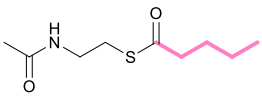 Exact mass = 204.1053 m/z (0.1 ppm)	⟹	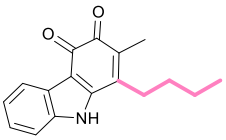 Exact mass = 268.1333 m/z (3.3 ppm)
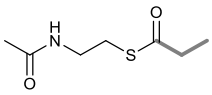 Exact mass = 176.0740 m/z (0.3 ppm)	⟹	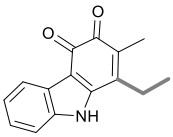 Exact mass = 240.1020 m/z (3.3 ppm)
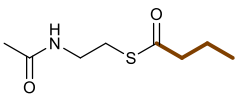 Exact mass = 190.0893 m/z (2.1 ppm)	⟹	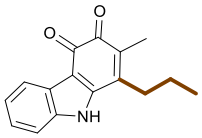 Exact mass = 254.1176 m/z (0.2 ppm)
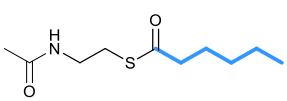 Exact mass = 218.1212 m/z (1.0 ppm)	⟹	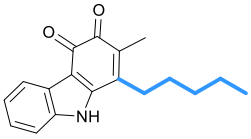 Exact mass = 282.1489 m/z (0.4 ppm)

Comparison of the ion intensities of these CA derivatives indicated that the addition of isovaleryl-SNAC and SNAC-related compounds into the three-enzyme system provided the best biotransformation outcome. As such, isovaleryl-SNAC was selected as the acyl donor for the subsequent studies.

It was confirmed that NzsH was able to convert indole-pyruvate derivatives with functionalized indole ring systems into the corresponding acyloins [24,25]. In this biotransformation system, the engineered tryptophan synthase *Pf*TrpB and a commercially available amino acid oxidase were used to convert indoles with structural diversity into their corresponding indole-pyruvates, which were subsequently converted into acyloins catalyzed by NzsH.

To investigate whether NzsJ and NzsI were able to convert these acyloins into the corresponding CAs, a one-pot reaction was performed in the presence of *Pf*TrpB, the L-amino acid oxidase (LAAO) from snake venom (Sigma Aldrich catalog number: A5147), and NzsH, together with the necessary reaction conditions and cofactors. In a control assay with boiled NzsJ or NzsI and in other control assays lacking either indole or SNAC substrate, the formation of isovaleryl-containing CA was not observed (Figure 3B(i)). The reaction was initiated by adding indole, L-Ser, and isovaleryl-SNAC. Isovaleryl-containing CA was generated with a m/z value of 268.1238, as observed in the HR-ESIMS analysis (Figure 3B(ii)).

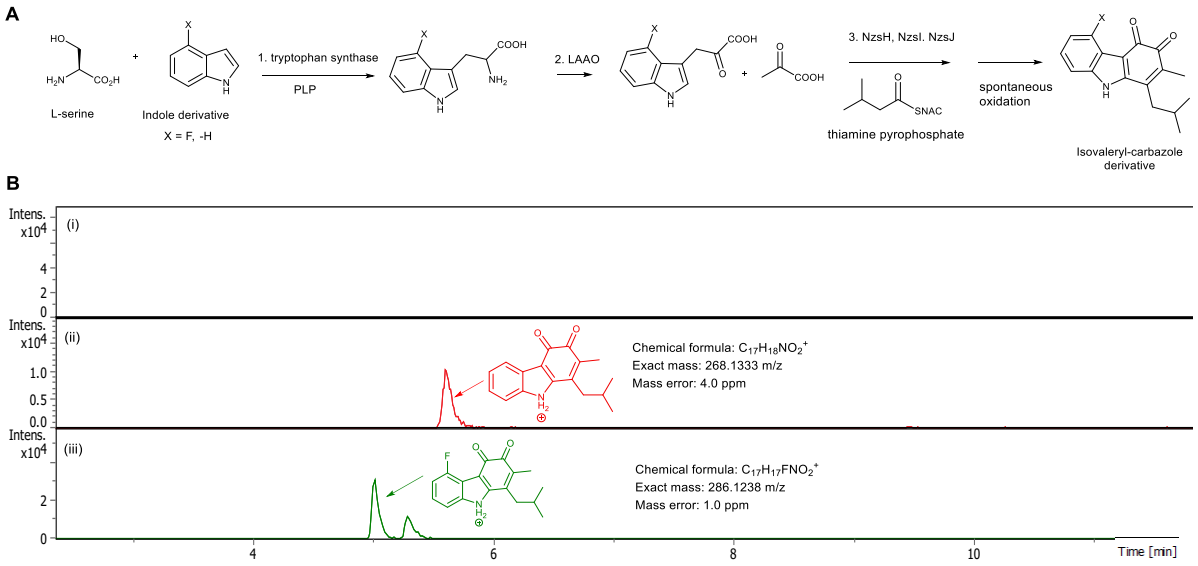

Figure 3. (**A**) One-pot 5-enzymatic system to generate isovaleryl-carbazole derivatives. (**B**) Extracted ion chromatography of HR-LCMS analysis confirming production of isovaleryl-carbazole (red) and 4-fluoro-isovaleryl carbazole (green). (i) the enzymatic system in the absence of indole as control; (ii) the enzymatic system in the presence of 4H-indole; (iii) the enzymatic system in the presence of 4-fluoro-indole.

This result further encouraged us to investigate whether other indole derivatives can enter the CA scaffolds. To do this, the biotransformation was carried out using the five-enzyme system together with various commercially available indoles, L-Ser, and isovaleryl-SNAC. Among the indole derivatives tested, only 4-fluoro-indole was able to be incorporated into the CA framework, as determined by HR-ESIMS analysis (Figure 3B(iii)).

Taken together, our studies demonstrated that NzsJ and NzsI, unlike the upstream enzyme NzsH, which displays considerable substrate tolerance toward indole ring systems, exhibit rather limiting substrate plasticity toward indole rings. The biotransformation developed here indicated that the catalytic capacities of NzsJ and NzsI are the key limiting factors in generating CAs with different substituents of indole rings. Further studies are required to improve the reactivities of NzsJ and NzsI enzymes towards unnatural indole

derivatives. This can be achieved via either identification of new NzsJ/NzsI homologues through comparative genomics or directed evolution to provide an engineered NzsJ/NzsI, with the aim of finding a suitable biocatalyst with better kinetics to efficiently generate structurally diverse CA derivatives.

In conclusion, two one-pot biotransformation systems were developed herein, a three-enzyme and a five-enzyme system, to access the synthetically challenging CA framework. The combination of NzsH, NzsJ, and NzsI, together with synthetic acyl SNAC surrogates, allowed the generation of CA derivatives with diverse acyl tails attached to the tricyclic carbazole scaffold. Among the acyl-SNACs examined, isovaleryl-SNAC appeared to be the best acyl donor for this three-enzyme system. Our biotransformation system was further expanded by including *Pf*TrpB, an L-amino acid oxidase (LAAO). Addition of various indole derivatives to this five-enzyme system indicated that only indole and 4-fluoro-indole were able to enter the synthetic pathway to deliver the corresponding CAs, suggesting a limited substrate tolerance toward the indole ring in the NzsJ/NzsI coupling reaction.

3. Methods and Materials

General chemicals, reagents, and analytical methods. All starting materials and reagents were purchased from commercial sources and used as received. All biochemical reactions, apart from where noted otherwise, were carried out in triplicate. Before every set of measurements, triplicate control reactions were performed to ensure that the assays were functioning correctly. All flash column chromatography was carried out using silica gel purchased from Sigma Aldrich, with the solvent systems noted. ^{19}F NMR spectra were recorded at 298 K on a Bruker Avance III 400 (BRUKER, Sylvenstein, Germany) using $CFCl_3$ as an external reference. Chemical shifts are reported in parts per million (ppm), and coupling constants (*J*) are reported in hertz (Hz).

Enzymatic assays were analyzed on an Agilent 1260 HPLC (Agilent, Stockport, UK) fitted with a C18 column pre-equilibrated with 20% B and developed at a flow rate of 0.8 mL/min: 0–35 min, a linear gradient from 80% A to 20% A; 20–25 min, a linear gradient from 80% A to 5% A; 25–27 min, constant with 5% A; 27–35 min, a linear gradient to 95% A; 30–35 min, constant with 80% A. Solvent A was 0.1% formic acid in water, and solvent B was 0.1% formic acid in acetonitrile.

Enzymatic reactions were also monitored with a Bruker MaXis II ESI-Q-TOF-MS connected to an Agilent 1290 Infinity II UHPLC fitted with a Phenomenex Kinetex XB-C18 (2.6 µM, 100 × 2.1 mm) column. The column was eluted with a linear gradient of 5–100% MeCN containing 0.1% formic acid over 15 min. The mass spectrometer (BRUKER, Sylvenstein, Germany) was operated in positive ion mode with a scan range of 200–3000 m/z. Source conditions were: end plate offset at −500 V; capillary at −4500 V; nebulizer gas (N_2) at 4.0 bar; dry gas (N_2) at 9.0 L min^{-1}; dry temperature at 200 °C. Ion transfer conditions were: ion funnel RF at 400 Vpp; multiple RF at 200 Vpp; quadrupole low mass at 200 m/z; collision energy at 8.0 eV; collision RF at 2000 Vpp; transfer time at 110.0 µs; pre-pulse storage time at 10.0 µs. MS data were analyzed using Bruker DataAnalysis (https://www.bruker.com/en.html, accessed on 15 August 2023) or Thermo Xcalibur (https://www.thermofisher.cn/order/catalog/product/OPTON-30965, accessed on 15 August 2023).

General methods of protein expression and purification. The synthetic constructs encoding NzsJ and NzsI were purchased from Genscript Ltd. and were individually transformed into *E. coli* BL21 (DE3). Single colonies from each transformation were grown overnight in LB media (5 mL) containing kanamycin (50 µg/mL) and chloramphenicol (25 µg/mL). The overnight culture was transferred to fresh LB medium (500 mL) supplemented with kanamycin (50 µg/mL) and cultivated at 37 °C until the cell density reached an OD_{600} of 0.6. IPTG was added to a final concentration of 0.1 mM to induce protein expression. Cells were grown for 16–20 h at 16 °C and then harvested by centrifugation at 4 °C. The cell pellets were resuspended in ice-cold lysis buffer (20 mM Tris-HCl, 300 mM NaCl, 10 mM imidazole, pH 8.0) and further disrupted using an ultrasonic homogenizer,

JY92-IIN (Thermo Scientific, Bremen, Germany). Then, the supernatant of cell debris was loaded onto a Ni-NTA-affinity column. Bound proteins were eluted with the same Tris-HCl buffer containing different concentrations of imidazole. The desired elution fractions were combined and concentrated using a centrifugal filter unit (Millipore, Gillingham, UK). The purification of recombinant NzsH and *Pf*TrpB was followed, as previously reported [24].

4. Biochemical Reactions

In the three-enzyme systems, a sample of NzsH (20 μM), NzsJ (40 μM), and NzsI (40 μM) was incubated with indole-3-pyruvate (1 mM), pyruvate (1 mM), and acyl-SNACs (1 mM) in phosphate buffer (50 mM, pH 7.5) to the final volume of 100 μL at 37 °C overnight, and then quenched by the addition of 100 μL of acetonitrile. The mixture was centrifuged at 13,000 rpm for 10 min. to remove protein precipitates.

To monitor the production of indole-containing acyloin derivatives, we followed an already developed and previously reported method [24]. Briefly, a sample of *Pf*TrpB^6 (20 μM) was incubated with indole or indole derivatives (1 mM), L-Ser (1 mM), and PLP (1 mM) in phosphate buffer (50 mM, pH 7.5) to a final volume of 100 μL at 37 °C for 3 h. To this mixture LAAO (20 μM) was added to a volume of 100 μL at 28 °C for another 1 h. Inclusion of NzsH (20 μM), TPP (1 mM), and Mg^{2+} (1 mM) into the mixture was performed to the final volume of 100 μL at 37 °C for 3 h. Because of the instability of acyloins, an overdose of $NaBH_4$ was added to the three-enzyme systems. Finally, the reaction mix was quenched by the addition of 100 μL of acetonitrile. The mixture was centrifuged at 13,000 rpm for 10 min. to remove protein precipitates.

In the five-enzyme systems, a sample of *Pf*TrpB (20 μM) was incubated with indole or indole derivatives (1 mM), L-Ser (1 mM), and PLP (1 mM) in phosphate buffer (50 mM, pH 7.5) to a final volume of 50 μL at 37 °C for 3 h. To this mixture, LAAO was added at 37 °C for another 1 h. Inclusion of NzsH (20 μM), NzsJ (40 μM) and NzsI (40 μM), TPP (1 mM), Mg^{2+} (1 mM), and isovaleryl-SNAC (1 mM) into the mixture was performed to the final volume of 100 μL at 37 °C overnight. The reaction mixture was then quenched by the addition of 100 μL of acetonitrile. The mixture was centrifuged at 13,000 rpm for 10 min. to remove protein precipitates.

Supplementary Materials: The following supporting information can be downloaded at: https://www.mdpi.com/article/10.3390/synbio2010002/s1. Figure S1: Acyl-SNAC species utilized in this study; Figure S2: SDS-PAGE electrophoresis analysis confirming correct expression and purity of protein TrpB (45.0 kDa), NzsH (64.0 kDa), NzsI (28.0 kDa), and NzsJ (35.0 kDa); Figure S3: HR-LCMS analysis confirming production of isovaleryl-carbazole; Figure S4: HR-LCMS analysis confirming production of acetyl-carbazole; Figure S5: HR-LCMS analysis confirming production of phenyl-carbazole; Figure S6: HR-LCMS analysis confirming production of phenyl-acetyl-carbazole; Figure S7: HR-LCMS analysis confirming production of decanoyl-carbazole; Figure S8: HR-LCMS analysis confirming production of isobutyryl-carbazole; Figure S9: HR-LCMS analysis confirming production of valeryl-carbazole; Figure S10: HR-LCMS analysis confirming production of propanoyl-carbazole; Figure S11: HR-LCMS analysis confirming production of butyl-carbazole; Figure S12: HR-LCMS analysis confirming production of hexyl-carbazole; Figure S13: 5-step one-pot enzymatic reaction and HR-LCMS analysis confirming production of 4-fluoro-isovaleryl-carbazole; Figure S14: 5-step one-pot enzymatic reaction and HR-LCMS analysis confirming production of isovaleryl-carbazole.

Author Contributions: Conceptualization, H.D. and K.K.; methodology, H.D.; software, F.C.; validation, S.A., F.C. and H.D.; formal analysis, F.C.; investigation, S.A.; resources, K.K.; data curation, F.C.; writing—original draft preparation, H.D.; writing—review and editing, H.D.; visualization, F.C.; supervision, H.D.; project administration, H.D.; funding acquisition, H.D. and K.K. All authors have read and agreed to the published version of the manuscript.

Funding: This research was funded by the College of Science and Arts, Jouf University, King Khaled Road, Kingdom of Saudi Arabia, and the Royal Embassy of Saudi Arabia Cultural Bureau in the UK for the PhD scholarship of S.A., the PhD studentship funded by IBioIC (F.C.), BBSRC (BB/R00479X/1), the National Natural Science Foundation of China (31929001), and the Royal Society-NSFC International Exchange Grant (IEC\NSFC\211349), the Leverhulme Trust-Royal Society Africa award (AA090088),

and the jointly funded UK Medical Research Council (MRC) and the UK Foreign, Commonwealth & Development Office (FCDO) under the MRC/FCDO Concordat agreement (MR/S00520X/1).

Institutional Review Board Statement: Not applicable.

Informed Consent Statement: Not applicable.

Data Availability Statement: Data is contained within the article or Supplementary Material.

Conflicts of Interest: The authors declare no conflicts of interest.

References

1. Lellouche, J.-P.; Koner, R.R.; Ghosh, S. N-Substituted Carbazole Heterocycles and Derivatives as Multipurpose Chemical Species: At the Interface of Chemical Engineering, Polymer and Materials Science. *Rev. Chem. Eng.* **2013**, *29*, 413–437. [CrossRef]
2. Kim, S.M.; Yun, J.H.; Han, S.H.; Lee, J.Y. A Design Strategy of Bipolar Host Materials for More than 30 Times Extended Lifetime in Phosphorescent Organic Light-Emitting Diodes Using Benzocarbazole and Quinazoline. *J. Mater. Chem. C* **2017**, *5*, 9072–9079. [CrossRef]
3. Nagase, Y.; Shirai, H.; Kaneko, M.; Shirakawa, E.; Tsuchimoto, T. Indium-Catalyzed Annulation of 3-Aryl- and 3-Heteroarylindoles with Propargyl Ethers: Synthesis and Photoluminescent Properties of Aryl- and Heteroaryl[c]Carbazoles. *Org. Biomol. Chem.* **2013**, *11*, 1456. [CrossRef]
4. Li, J.; Grimsdale, A.C. Carbazole-Based Polymers for Organic Photovoltaic Devices. *Chem. Soc. Rev.* **2010**, *39*, 2399. [CrossRef] [PubMed]
5. Hendsbee, A.D.; Sun, J.-P.; Law, W.K.; Yan, H.; Hill, I.G.; Spasyuk, D.M.; Welch, G.C. Synthesis, Self-Assembly, and Solar Cell Performance of N-Annulated Perylene Diimide Non-Fullerene Acceptors. *Chem. Mater.* **2016**, *28*, 7098–7109. [CrossRef]
6. Schmidt, A.W.; Reddy, K.R.; Knölker, H.-J. Occurrence, Biogenesis, and Synthesis of Biologically Active Carbazole Alkaloids. *Chem. Rev.* **2012**, *112*, 3193–3328. [CrossRef] [PubMed]
7. Pearce, C.J.; Doyle, T.W.; Forenza, S.; Lam, K.S.; Schroeder, D.R. The Biosynthetic Origins of Rebeccamycin. *J. Nat. Prod.* **1988**, *51*, 937–940. [CrossRef] [PubMed]
8. Takada, K.; Kajiwara, H.; Imamura, N. Oridamycins A and B, Anti-Saprolegnia Parasitica Indolosesquiterpenes Isolated from *Streptomyces* sp. KS84. *J. Nat. Prod.* **2010**, *73*, 698–701. [CrossRef]
9. Ding, L.; Maier, A.; Fiebig, H.-H.; Lin, W.-H.; Hertweck, C. A Family of Multicyclic Indolosesquiterpenes from a Bacterial Endophyte. *Org. Biomol. Chem.* **2011**, *9*, 4029. [CrossRef]
10. Ding, L.; Münch, J.; Goerls, H.; Maier, A.; Fiebig, H.-H.; Lin, W.-H.; Hertweck, C. Xiamycin, a Pentacyclic Indolosesquiterpene with Selective Anti-HIV Activity from a Bacterial Mangrove Endophyte. *Bioorg. Med. Chem. Lett.* **2010**, *20*, 6685–6687. [CrossRef]
11. Feng, N.; Ye, W.; Wu, P.; Huang, Y.; Xie, H.; Wei, X. Two New Antifungal Alkaloids Produced by Streptoverticillium Morookaense. *J. Antibiot.* **2007**, *60*, 179–183. [CrossRef] [PubMed]
12. Kato, S.; Kawai, H.; Kawasaki, T.; Toda, Y.; Urata, T.; Hayakawa, Y. Studies on Free Radical Scavenging Substances from Microorganisms. I. Carazostatin, a New Free Radical Scavenger Produced by Streptomyces Chromofuscus DC 118. *J. Antibiot.* **1989**, *42*, 1879–1881. [CrossRef] [PubMed]
13. Kato, S.; Shindo, K.; Kataoka, Y.; Yamagishi, Y.; Mochizuki, J. Studies on Free Radical Scavenging Substances from Microorganisms. II. Neocarazostatins A, B and C, Novel Free Radical Scavengers. *J. Antibiot.* **1991**, *44*, 903–907. [CrossRef]
14. Nakamura, S. New Antibiotics, Carbazomycins A and B. II. Structural Elucidation. *J. Antibiot.* **1980**, *33*, 961–966.
15. Tanaka, M.; Shin-Ya, K.; Furihata, K.; Seto, H. Isolation and Structural Elucidation of Antioxidative Substances, Carbazoquinocins A to F. *J. Antibiot.* **1995**, *48*, 326–328. [CrossRef] [PubMed]
16. Shin-ya, K.; Kunigami, T.; Kim, J.-S.; Furihata, K.; Hayakawa, Y.; Seto, H. Carquinostatin B, a New Neuronal Cell-Protecting Substance Produced by *Streptomyces exfoliatus*. *Biosci. Biotechnol. Biochem.* **1997**, *61*, 1768–1769. [CrossRef]
17. Huang, S.; Elsayed, S.S.; Lv, M.; Tabudravu, J.; Rateb, M.E.; Gyampoh, R.; Kyeremeh, K.; Ebel, R.; Jaspars, M.; Deng, Z.; et al. Biosynthesis of Neocarazostatin A Reveals the Sequential Carbazole Prenylation and Hydroxylation in the Tailoring Steps. *Chem. Biol.* **2015**, *22*, 1633–1642. [CrossRef]
18. Su, L.; Zhang, R.; Kyeremeh, K.; Deng, Z.; Deng, H.; Yu, Y. Dissection of the Neocarazostatin: A C_4 Alkyl Side Chain Biosynthesis by in Vitro Reconstitution. *Org. Biomol. Chem.* **2017**, *15*, 3843–3848. [CrossRef]
19. Su, L.; Lv, M.; Kyeremeh, K.; Deng, Z.; Deng, H.; Yu, Y. A ThDP-Dependent Enzymatic Carboligation Reaction Involved in Neocarazostatin A Tricyclic Carbazole Formation. *Org. Biomol. Chem.* **2016**, *14*, 8679–8684. [CrossRef]
20. Kobayashi, M.; Tomita, T.; Shin-ya, K.; Nishiyama, M.; Kuzuyama, T. An Unprecedented Cyclization Mechanism in the Biosynthesis of Carbazole Alkaloids in *Streptomyces*. *Angew. Chem. Int. Ed.* **2019**, *58*, 13349–13353. [CrossRef]
21. Liu, Y.; Su, L.; Fang, Q.; Tabudravu, J.; Yang, X.; Rickaby, K.; Trembleau, L.; Kyeremeh, K.; Deng, Z.; Deng, H.; et al. Enzymatic Reconstitution and Biosynthetic Investigation of the Bacterial Carbazole Neocarazostatin A. *J. Org. Chem.* **2019**, *84*, 16323–16328. [CrossRef] [PubMed]
22. Shen, Y.; Zhang, L.; Yang, M.; Shi, T.; Li, Y.; Li, L.; Yu, Y.; Deng, H.; Lin, H.-W.; Zhou, Y. Switching Prenyl Donor Specificities in Squalene Synthase-Like Aromatic Prenyltransferases from Bacterial Carbazole Alkaloid Biosynthesis. *ACS Chem. Biol.* **2023**, *18*, 123–133. [CrossRef] [PubMed]

23. Nagata, R.; Suemune, H.; Kobayashi, M.; Shinada, T.; Shin-ya, K.; Nishiyama, M.; Hino, T.; Sato, Y.; Kuzuyama, T.; Nagano, S. Structural Basis for the Prenylation Reaction of Carbazole-Containing Natural Products Catalyzed by Squalene Synthase-Like Enzymes. *Angew. Chem. Int. Ed.* **2022**, *61*, e202117430. [CrossRef] [PubMed]
24. Alrashdi, S.; Casolari, F.; Alabed, A.; Kyeremeh, K.; Deng, H. Chemoenzymatic Synthesis of Indole-Containing Acyloin Derivatives. *Molecules* **2023**, *28*, 354. [CrossRef]
25. Maglangit, F.; Alrashdi, S.; Renault, J.; Trembleau, L.; Victoria, C.; Tong, M.H.; Wang, S.; Kyeremeh, K.; Deng, H. Characterization of the Promiscuous *N*-Acyl CoA Transferase, LgoC, in Legonoxamine Biosynthesis. *Org. Biomol. Chem.* **2020**, *18*, 2219–2222. [CrossRef]
26. Casolari, F.; Alrashdi, S.; Carr, R.; Deng, H. Exploring a *Streptomyces* Wax Synthase Using Acyl-SNACs as Donor Substrates. *RSC Chem. Biol.* **2023**, *4*, 742–747. [CrossRef]